

RESEARCH

Open Access



# Preparation and characterization of self-aggregating micelles from stearic acid-modified burdock root polysaccharide

Chenchen Zhang<sup>1†</sup>, Hongjuan Wang<sup>2†</sup>, Yan Zhang<sup>1</sup>, Jiangfeng Song<sup>1,2\*</sup>  and Ying Li<sup>1</sup>

## Abstract

In order to obtain amphiphilic polysaccharide self-assembly micelles, the hydrophobic modification by grafting stearic acid (SA) onto the backbone of burdock root polysaccharide (BRP) was carried out and its main physicochemical properties were characterized. The results showed that the optimal esterification conditions were as follows: reaction time of 2 h, reaction temperature of 55 °C, system pH of 8.0 and the SA addition of 4 mmol, a maximum substitution degree (DS) of the esterification products was obtained as 0.1012. The FTIR analysis verified that the modified polysaccharide successfully introduced the ester carbonyl group. <sup>1</sup>H NMR spectra further confirmed that the esterification reaction occurred. The SA-modified BRP micelles were roughly spherical with uniform dispersion and the particle size was in the range of 259–352 nm, which showed a negative correlation with the DS. The solubility of the esterification products also decreased. The smaller critical micelle concentration (CMC) led to easier formation of self-aggregating micelles and stronger solubilization effect. The above results indicated that SA-modified BRP as a novel carrier material possessed potential to deliver hydrophobic active substances.

**Keywords** Burdock root polysaccharide, Stearic acid, Modification, Self-aggregating micelles

<sup>†</sup>Chenchen Zhang and Hongjuan Wang are co-first authors.

\*Correspondence:

Jiangfeng Song

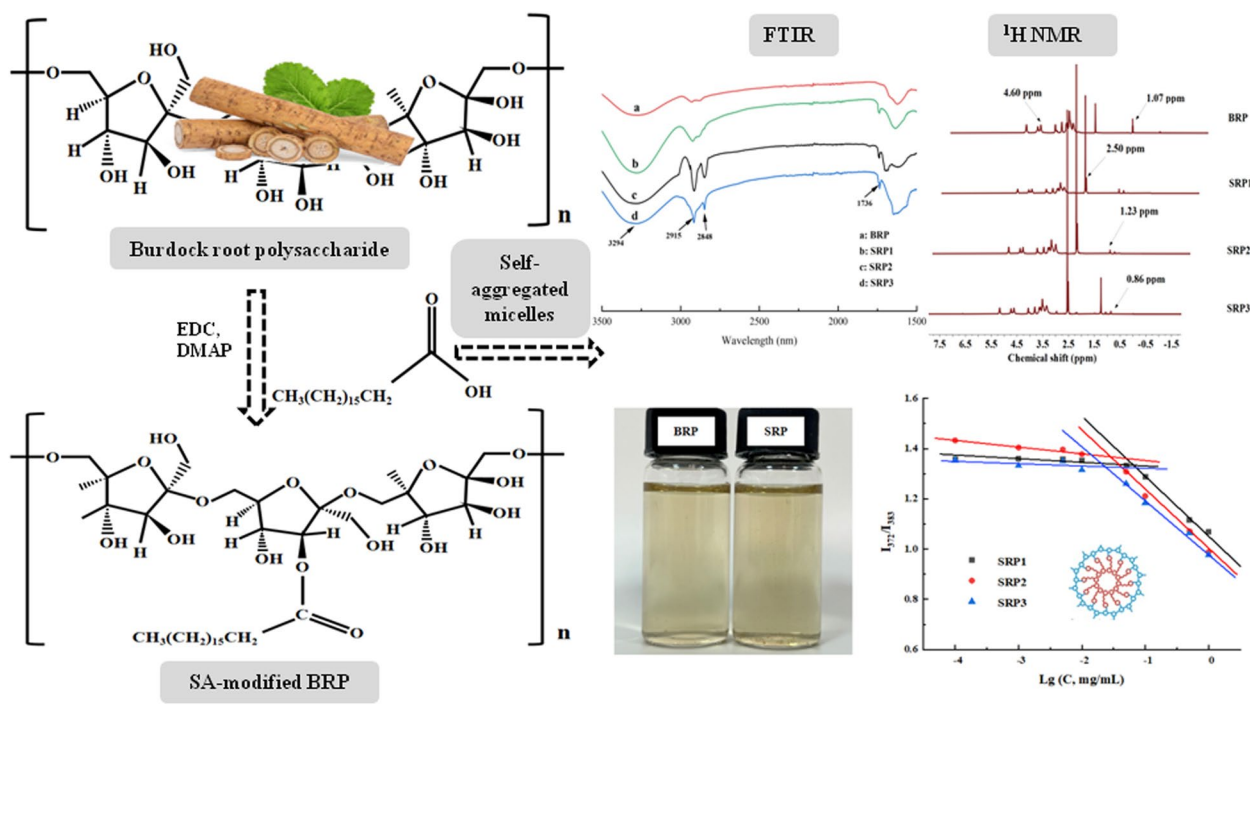
[songjiangfeng102@163.com](mailto:songjiangfeng102@163.com)

Full list of author information is available at the end of the article



© The Author(s) 2024. **Open Access** This article is licensed under a Creative Commons Attribution 4.0 International License, which permits use, sharing, adaptation, distribution and reproduction in any medium or format, as long as you give appropriate credit to the original author(s) and the source, provide a link to the Creative Commons licence, and indicate if changes were made. The images or other third party material in this article are included in the article's Creative Commons licence, unless indicated otherwise in a credit line to the material. If material is not included in the article's Creative Commons licence and your intended use is not permitted by statutory regulation or exceeds the permitted use, you will need to obtain permission directly from the copyright holder. To view a copy of this licence, visit <http://creativecommons.org/licenses/by/4.0/>.

## Graphical Abstract



## Introduction

In recent years, the application of amphiphilic polymer micelles in the fields of food and biomedicine has become increasingly widespread, with hydrophobic modified polysaccharide self-aggregating micelles being the most typical (Perumal et al. 2022). Amphiphilic polysaccharides can spontaneously form inner hydrophobic and outer hydrophilic micelles in aqueous media. Their unique structure endows them with excellent performance in solubilization, targeted transportation, controlled release, bioavailability improvement and stabilization of hydrophobic drugs or active substances (Bu et al. 2021). According to the source, amphiphilic polymers are divided into modified natural polymers (such as carboxymethyl starch) and synthetic polymers (such as polyoxyethylene-poly(lactic acid) copolymers). The modified natural polymers introduce hydrophobic groups through specific chemical reactions such as esterification, etherification, and reductive amination to synthesize amphiphilic products (Ma et al. 2016).

Plant polysaccharides have become excellent natural materials for the preparation of hydrophobically-modified

amphiphilic polymers due to their abundant sources, non-toxicity, good biocompatibility, biodegradability, and easy structural modification (Shah et al. 2018). The hydroxyl groups of natural polysaccharides (such as dextran and fructan) can react with various organic acids and their derivatives (such as stearic acid, octenyl succinic acid and dodecyl succinate) to obtain hydrophobically-modified amphiphilic products. Liu et al. (2022) modified fenugreek galactomannan via an electrophilic addition reaction with octenyl succinic anhydride, and systematically studied the parameters affecting the esterification reaction. Li et al. (2019) esterified quinoa starch granules with dodecyl succinic anhydride to various degrees of substitution, investigated the physicochemical properties and emulsification capacity of the modified starch. As an endogenous long-chain saturated fat acid, stearic acid (SA) is commonly used for the modification of polysaccharide materials due to its low cytotoxicity, high biocompatibility, strong photothermal stability and the role of a surfactant, which has been grafted onto different polysaccharides such as glucan, chitosan, pullulan and hyaluronic acid (Yang et al. 2021; Hu et al. 2006; Wang

et al. 2012; Jeong et al. 2019). Wang et al. (2012) found that the uptake efficiency of SA-modified biocompatible pullulan derivatives/doxorubicine was rather higher than that of free doxorubicine. The result of Jeong et al. (2019) suggested that hyaluronic acid-g-SA nanoparticles be expected to have high therapeutic efficacy for enabling targeted drug delivery and rapid release. SA-modified polysaccharide micelles improved the bioavailability of some drugs or physiologically active substances, which provided more operability for designing new polysaccharide micelles.

Burdock (*Arctium lappa* L.) is a biennial herb of the compositae family (Jin et al. 2023). As a plant with the same source of medicine and food, burdock root has been recognized as a health food and is increasingly favored by consumers. It is rich in polysaccharides, proteins, phenolics, calcium, phosphorus, iron and other minerals (Jin et al. 2023). Burdock root polysaccharide (BRP) has good water solubility and is a kind of resistant fructooligosaccharide. It has a variety of biological activities such as regulating gut microbiota, reducing blood sugar and blood lipids, and inhibiting tumor cell growth (Li et al. 2021). Presently, many studies on BRP primarily focuses on its extraction, purification, and physicochemical analysis (Jiang et al. 2019; Wang et al. 2023). Amphiphilic BRPs could be obtained by a moderate hydrophobic modification through changing its molecular structure, physicochemical and functional characteristics. It may exhibit better compatibility with the body, interact better with nutrients or various enzymes, and thus enhance the utilization of active substances (Yang et al. 2021).

In this study, SA was therefore conducted to synthesize amphiphilically-modified BRP, and the effects of different

preparation conditions on the substitution degree (DS) of modified BRP were investigated. The structure of the esterified products was characterized by FTIR spectroscopy and  $^1\text{H}$  NMR. The solubility, particle size, zeta potential, critical micelle concentration (CMC), and microstructure of the modified polysaccharide were analyzed to provide a reference for its application as a delivery carrier of hydrophobic active substances.

## Materials and methods

### Materials

Burdock root polysaccharide (BRP), purity > 85%, self-made in the laboratory; 1-(3-dimethylaminopropyl)-3-ethylcarbodiimide hydrochloride (EDC), 4-dimethylaminopyridine (DMAP) and stearic acid (SA) were analytically pure, which were purchased from Shanghai Maclean Biochemical Technology Co., Ltd. (Shanghai, China); dimethyl sulfoxide (DMSO) was analytically pure, which was obtained from Sinopharm Chemical Reagent Co., Ltd. (Shanghai, China); pyrene was analytically pure, which was purchased from Tianjin Xi'ensi Biochemical Technology Co., Ltd. (Tianjin, China); the molecular weight cut off (MWCO) of the dialysis bag was 8000–12,000 Da; deionized water, self-made in the laboratory.

### Synthesis of SA-modified BRP

The purified BRP from our laboratory was a furan type polysaccharide, which was mainly composed of five monosaccharides: fructose, glucose, arabinose, galactose and glucosamine hydrochloride. The molar ratio was 0.844: 0.122: 0.024: 0.008: 0.002, of which fructose accounted for more than 80%. The synthesis of SA-modified BRP mainly referred to the method of Wang et al. (2012) with slight modifications.

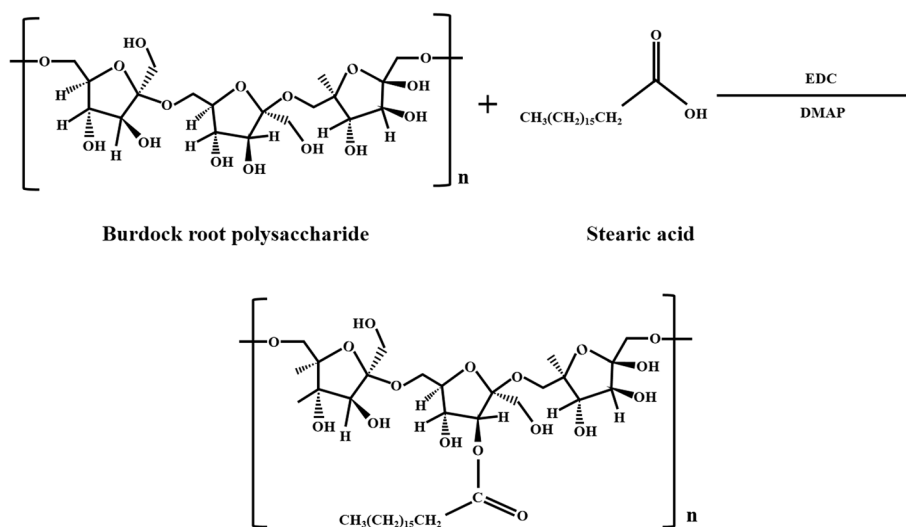


**Fig. 1** SA-modified BRP polymer synthesis route

The hydrophobic side of SA was linked to the backbone of BRP using EDC and DMAP as catalysts. The experimental synthesis route was shown in Fig. 1. 3.0 g BRP was accurately weighed and dissolved in 20 mL DMSO. 1.0–3.0 mmol SA was added to DMAP and EDC (SA: DMAP: EDC = 1:1:1.2, molar ratio), and dissolved in 3 mL DMSO, stirred and activated for 1–3 h. The activation solution was slowly added to the BRP solution under magnetic stirring, and reacted for 48 h at 25 °C. The reaction solution was added drop by drop into absolute ethanol to precipitate. The white precipitate was collected and re-dispersed in double distilled water, and transferred into dialysis bag (MWCO: 8000–12,000 Da) for dialysis. The samples were collected after dialysis for freeze drying.

#### Determination of degree of substitution in SA-modified BRP

The degree of substitution (DS) was determined according to the method of Varavinit et al. (2001) with slight modifications. 5 g SA-modified BRPs with different DS were placed in a 250 mL conical flask, 100 mL ethanol with a volume fraction of 80% was added to remove unreacted SA, and placed in a water bath at 50 °C. After being stirred for 15 min, the sample was poured into the funnel, washed three times with 80% ethanol at 50 °C, filtered until there was no chloride ion in the sample solution (tested with silver nitrate solution), and finally the sample was finally freeze-dried.

1 g of the above sample was placed in a 250 mL Erlenmeyer flask, 50 mL of deionized water was added, and then 20 mL of 0.25 mol/L NaOH solution was added, placed on a constant temperature shaking shaker at 37 °C for 1 h, then two drops of phenolphthalein indicator were added, and the solution was titrated with 0.1 mol/L HCl until the pink color just disappeared, and the volume  $V_1$  of HCl consumed by titration was recorded. The unmodified BRP was used as the blank control. The DS of SA-modified BRP was calculated according to the formula (1).

$$DS = \frac{162 \times C(V_0 - V_1)}{1000m - 266 \times C(V_0 - V_1)} \quad (1)$$

Where  $V_0$ - volume of HCl required to titrate the unmodified sample, mL;  $V_1$ - volume of HCl required for titrating the modified sample to be tested, mL; C - molar concentration of standard HCl, mol/L; m: sample mass, g; 162- molar molecular weight of dehydrated glucose unit; 266- molar molecular weight of stearyl  $\text{CH}_2(\text{CH}_2)_{16}\text{CO}$ .

#### FTIR measurement

The spectra of SA-modified BRPs were obtained with a fourier-transform infrared (FTIR) spectrometer (Nicolet iS50, Thermo Fisher, Madison, USA). After deducting the air background, 10 mg BRP and their modified polysaccharides with different DS were freeze-dried and placed on crystals with attenuated total reflection (ATR) attachment. The samples were compacted and scanned within the range of  $4000 - 500 \text{ cm}^{-1}$ , with 32 scans and a resolution of  $4 \text{ cm}^{-1}$ .

#### $^1\text{H}$ NMR determination

10 mg BRP and SA-modified BRPs freeze-dried samples were accurately weighed and placed in nuclear magnetic resonance tubes, and completely dissolved by DMSO- $d_6$ , the sample testing temperature was set to 25 °C, scanned at 64 times/min, and performed conformational analysis by  $^1\text{H}$  nuclear magnetic resonance (NMR) spectroscopy (AVANCE III 600 MHz spectrometer, Bruker Biospin, Switzerland).

#### Determination of solubility of SA-modified BRP

According to the method of Song et al. (2016), 0.2 g BRP and their derivatives were dissolved in 10 mL of double distilled water, transferred to a known constant weight glass centrifuge tube, centrifuged at 5000 rpm for 10 min, and the supernatant was collected and dried at 105 °C to constant weight. The solubility formula (2) was as follows.

$$\text{Solubility} = \frac{\text{Mass of supernatant after drying (g)}}{\text{Original sample gross weight (g)}} \times 100\% \quad (2)$$

#### Preparation of self-aggregating micelles of SA-modified BRP

SA-modified BRP micelles were prepared using the dialysis method (Chen et al. 2011). 300 mg of SA-modified BRP samples with different degrees of substitution were dissolved in 3 mL DMSO, stirred on a magnetic stirrer until completely dissolved, transferred to a dialysis bag (MWCO: 8000–12,000), and dialyzed in 1 L double distilled water for 48 h. In the first 12 h, the water was changed every 3 h, and then every 8 h. After the DMSO was thoroughly dialyzed, the solution was taken out to 100 mL, and treated in a ultrasonic instrument (FS-150 N, Shanghai Shengxi Ultrasonic Instrument Co., Ltd., Shanghai, China) with a power of 80 W for 3 min, then filtered with a  $0.45 \mu\text{m}$  filter membrane to obtain self-assembled micelles, and store in a 4 °C refrigerator for later use.

### Determination of critical micelle concentration

Critical micelle concentration (CMC) was determined by a fluorescent probe method (Yan et al. 2019). 20  $\mu\text{L}$  of  $3 \times 10^{-4}$  mol/L pyrene methanol solution was added to a 10 mL stoppered test tube, the methanol was blown dry with liquid nitrogen, then 10 mL of SA-modified BRP micellar solution with different concentrations (0.0003–3 mg/mL) was added, the final concentration of pyrene was adjusted to  $6 \times 10^{-7}$  mol/L. The mixture solution was stood for 1 h to fully dissolve pyrene into the hydrophobic inner core, and evenly distributed with a vortex oscillator. After being kept overnight in dark, the sample was transferred to a 96-well plate, and the emission spectrum of pyrene was measured with a fluorescence spectrophotometer (LS55, PerkinElmer, Waltham, MA). The excitation wavelength was set to 334 nm, the width of the emission and excitation slits were both 10 nm, and the scanning range of the emission spectrum was 350–450 nm. The fluorescence intensities of  $I_{372}$  and  $I_{383}$  were recorded, and the CMC was calculated by plotting the  $I_{372}/I_{383}$  of pyrene against  $\text{Lg}(C)$  of the mass concentration of SA-modified BRP.

### Particle size and zeta potential measurement

The particle size and polydispersity index (PDI) of SA-modified BRP self-assembled micelles were determined by dynamic light scattering (DLS) (NICOMP Z3000, PSS particle size analyzer, USA). The micelle solution concentration was 2 mg/mL. The zeta potential of these micelles was measured using the same equipment. DLS measurement conditions: room temperature, the light scattering angle was  $90^\circ$ , the output power was 30 W, the viscosity was 0.933 cP, and the refractive index of reference was 1.333.

### Transmission electron microscopy observation

According to the method of Liu et al. (2016), a JEM-1200EX transmission electron microscope (TEM, JEOL Ltd., Japan) was used to observe the morphology of SA-modified BRP micelles with different degrees of substitution. Polysaccharide micelles at a concentration of 2 mg/mL were dropped on the copper film grid stained with phosphotungstic acid, and observed by transmission electron microscopy (TEM) after drying.

### Statistics analysis

The experiments were repeated three times, and the results were expressed as mean  $\pm$  standard deviation (SD). Statistical analysis was performed using analysis of variance (ANOVA) followed by Duncan's test. A value of  $p < 0.05$  was considered statistically significant.

## Results and discussion

### The effects of reaction conditions on the DS of esterification products

The amphiphilic BRP derivatives were synthesized through the reaction between the carboxylic groups of SA and the hydroxyl groups of BRP. The effect of different reaction temperatures on the DS of the esterification product was investigated. As presented in Fig. 2A, the fixed SA addition was 1 mmol, system pH value was 7.0 and reaction time was 2 h, when the reaction temperature was  $55^\circ\text{C}$ , the DS of the esterification product reached the maximum. In the range of  $25 \sim 55^\circ\text{C}$ , with the rise of the reaction temperature, the thermal motion between polysaccharide and SA molecules intensified, which increased the number of effective collisions between molecules, leading to an increase in the reaction rate. If the reaction temperature continued to rise, the hydrolysis rate of SA would increase, and the esterification product might decompose, thus the DS decreased. Li et al. (2020) and Chang et al. (2014) also observed a similar phenomenon in the preparation of modified starch.

The effect of reaction time was investigated with a fixed SA addition at 1 mmol, system pH of 7.0 and reaction temperature of  $55^\circ\text{C}$ . As shown in Fig. 2B, as reaction time increased, the DS of the esterification product gradually increased, and the esterification reaction gradually reached its limit value with the extension of time. After more than 2 h, the DS of the product gradually decreased. This was because in the early stage, the esterification reaction between BRP and SA proceeded in a positive direction. If the reaction time continued to extend, it might lead to the decomposition of the esterification product, making the synthesis rate of the product be smaller than the decomposition rate, thus the reaction could not be extended indefinitely.

The effect of system pH on the DS of the esterification product was investigated. As shown in Fig. 2C, the fixed SA addition was 1 mmol, the reaction temperature was  $55^\circ\text{C}$  and reaction time was 2 h, within the system pH range of 6–10, the esterification products gradually increased with the increase of pH. The maximum DS was 0.0256 when the system pH value was 8.0. The possible reason was that when the system pH value was less than 8.0, the hydroxyl activity of BRP in the reaction system was weak, making it difficult to undergo esterification reaction with SA and resulting in a lower DS; When the pH value was above 8.0, it was easy to cause the hydrolysis of SA and BRP, resulting in a decrease in DS.

The effect of different SA additions on the DS of the esterification product was investigated. As presented in Fig. 2D, the fixed system pH value was 8.0, the reaction temperature was  $55^\circ\text{C}$  and reaction time was 2 h,

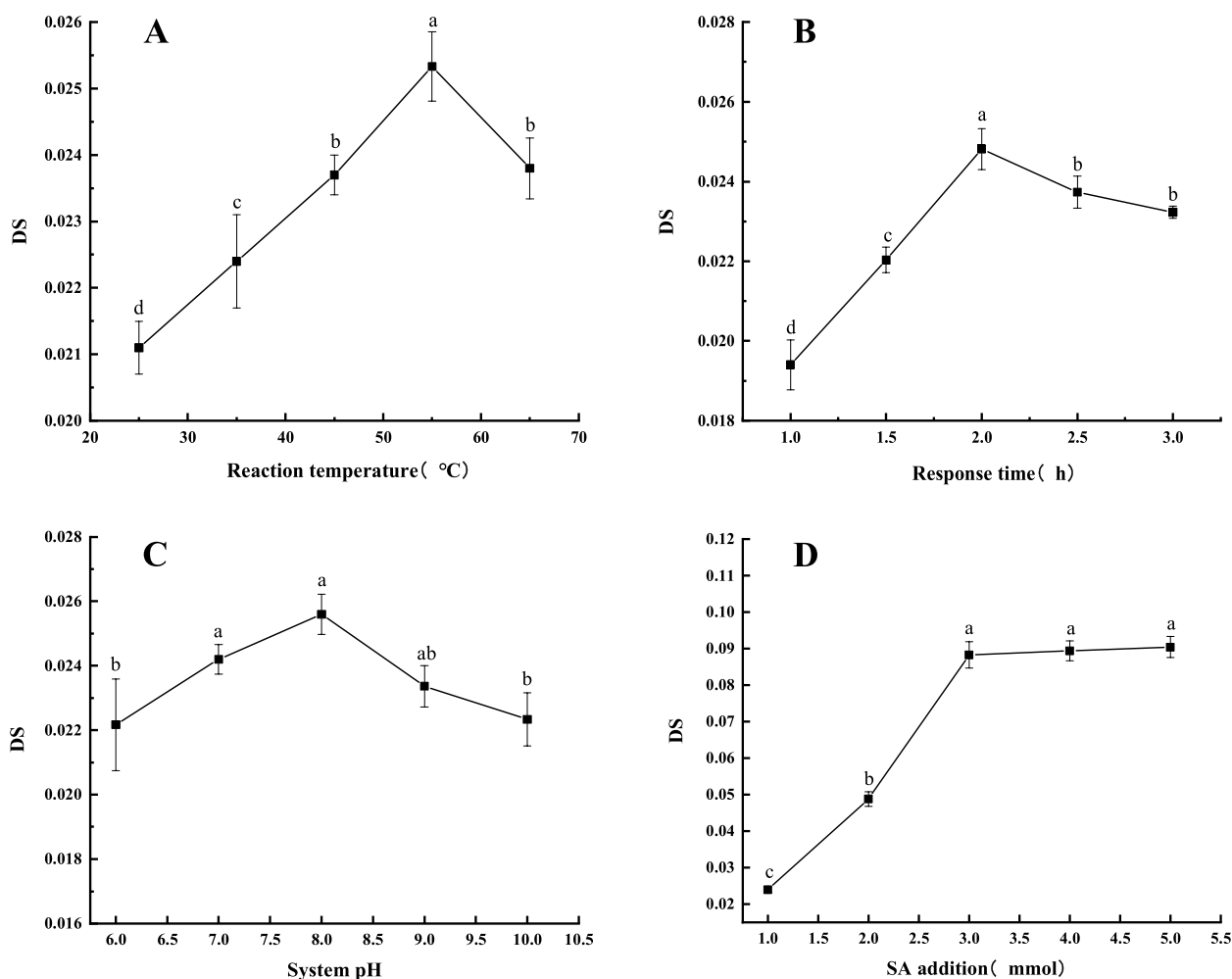


**Fig. 2** The effects of reaction conditions on the DS of the esterification products. Different lowercase letters indicate significant differences between groups ( $p < 0.05$ )

when the amount of SA added increased from 1 mmol to 3 mmol, the DS of the esterification products gradually increased, reaching the maximum of 0.0883. When the amount of SA continued to increase, the increasing trend of DS slowed down. The reason might be that as the amount of SA increased, the collision frequency between BRP and SA molecules increased, increasing the probability of esterification reaction (Lin et al. 2019), and excessive SA would tend to saturate the reaction.

#### Optimization of preparation conditions for SA-modified BRP

The orthogonal design of experiments was carried out by using SPSS 25 software. The effects of reaction temperature (A), reaction time (B), system pH (C) and SA addition (D) on the DS of SA-modified BRP were further

studied by four factors and three levels, and the optimal preparation conditions were determined. The selected variables and their experimental levels were as follows: A of 45 to 65, B of 1.5 to 2.5, C of 7 to 9, and D of 2 to 4. The range results in Table 1 indicated that the order of importance of each independent factor was  $D > B > A > C$ . Therefore, the amount of SA added had the greatest impact on DS, followed by the reaction time and temperature, and the system pH had the smallest impact. From the K value levels of each factor, it could be inferred that the optimal level was  $A_2B_2C_2D_3$ . Based on the analysis of variance (Table 2), the addition of SA ( $p < 0.01$ ), reaction temperature ( $p < 0.05$ ) and reaction time ( $p < 0.05$ ) had a significant impact on the DS, while the system pH showed no significant difference. Validation experiments were further conducted under the optimal conditions to verify the adequacy of the test results, the corresponding

**Table 1** Orthogonal test results of SA-modified BRP preparation conditions

No.	Factors				DS
	A: Reaction temperature (°C)	B: Reaction time (h)	C: System pH	D: SA addition (mmol)	
1	45	1.5	7	2	0.0361 ± 0.0012
2	45	2.0	8	3	0.0842 ± 0.0033
3	45	2.5	9	4	0.0857 ± 0.0018
4	55	1.5	8	4	0.0765 ± 0.0022
5	55	2.0	9	2	0.0494 ± 0.0016
6	55	2.5	7	3	0.0833 ± 0.0032
7	65	1.5	9	3	0.0539 ± 0.0024
8	65	2.0	7	4	0.0761 ± 0.0028
9	65	2.5	8	2	0.0382 ± 0.0017
K <sub>1</sub>	0.2060	0.1665	0.1955	0.1237	
K <sub>2</sub>	0.2092	0.2097	0.1989	0.2214	
K <sub>3</sub>	0.1682	0.2072	0.1890	0.2383	
k <sub>1</sub>	0.0687	0.0555	0.0652	0.0412	
k <sub>2</sub>	0.0697	0.0699	0.0663	0.0738	
k <sub>3</sub>	0.0561	0.0691	0.0630	0.0794	
R	0.0137	0.0144	0.0033	0.0382	

**Table 2** Variance analysis of orthogonal test

Factors	Sum of square	Degree of freedom	Mean of square	F	P	Significant
A	0.000347	2	0.000173	20.551	0.046	*
B	0.000392	2	0.000196	23.245	0.041	*
C	0.000017	2	0.000008	1.000	0.500	
D	0.002552	2	0.001276	151.258	0.007	**
Error	0.000017	2	0.000008			
Total	0.003308	8				

\*\*: $p < 0.01$ ; \*: $p < 0.05$

DS was found close to the orthogonal test value. Namely, when the amount of SA added was 4.0 mmol, the reaction temperature was 55 °C, the reaction time was 2.0 h and the system pH value was 8, there was a maximum DS of 0.1012.

#### FTIR analysis

As shown in Fig. 3A, it was evident that the infrared spectra of BRP after hydrophobic modification with SA showed an enhanced absorption peak at 3294  $\text{cm}^{-1}$  compared to the original BRP, indicating that hydroxyl groups in the polysaccharides might be involved in chemical reactions. The absorption peaks caused by C-H stretching vibration at 2915  $\text{cm}^{-1}$  and 2848  $\text{cm}^{-1}$  were obviously enhanced. Moreover, a new peak generated by ester carbonyl vibration appeared at 1736  $\text{cm}^{-1}$ , and the intensity of this peak increased with the increase of DS (Yang et al. 2022). This proved that the BRP after hydrophobic

modification with SA introduced ester carbonyl groups, thereby verifying the esterification reaction between BRP and SA.

#### <sup>1</sup>H NMR analysis

Figure 3B exhibited the <sup>1</sup>H NMR of BRP and SA-modified BRP with different DS (DMSO d<sub>6</sub> with TMS, ppm). Comparing the spectra of relevant literature (Lu et al. 2013), it could be seen that  $\delta$  4.6 ppm reflected the proton peak of  $\alpha(1-6)$  H on the BRP,  $\delta$  5.05 ppm was the isomeric proton peak of  $\alpha(1-4)$ H on the BRP, The proton peak near  $\delta$  2.50 ppm was the solvent peak of DMSO-S<sub>6</sub>, the peak near  $\delta$  3.37 ppm was the proton peak of water, and the methyl peak adjacent to the non-polar functional group was reflected at  $\delta$  1.07 ppm. Compared with BRP, there was a new peak in <sup>1</sup>H NMR after SA modification,  $\delta$  1.23 ppm corresponded to the proton peak of  $-\text{CH}_2$  on SA, and the three hydrogens of the methyl group at the end of the

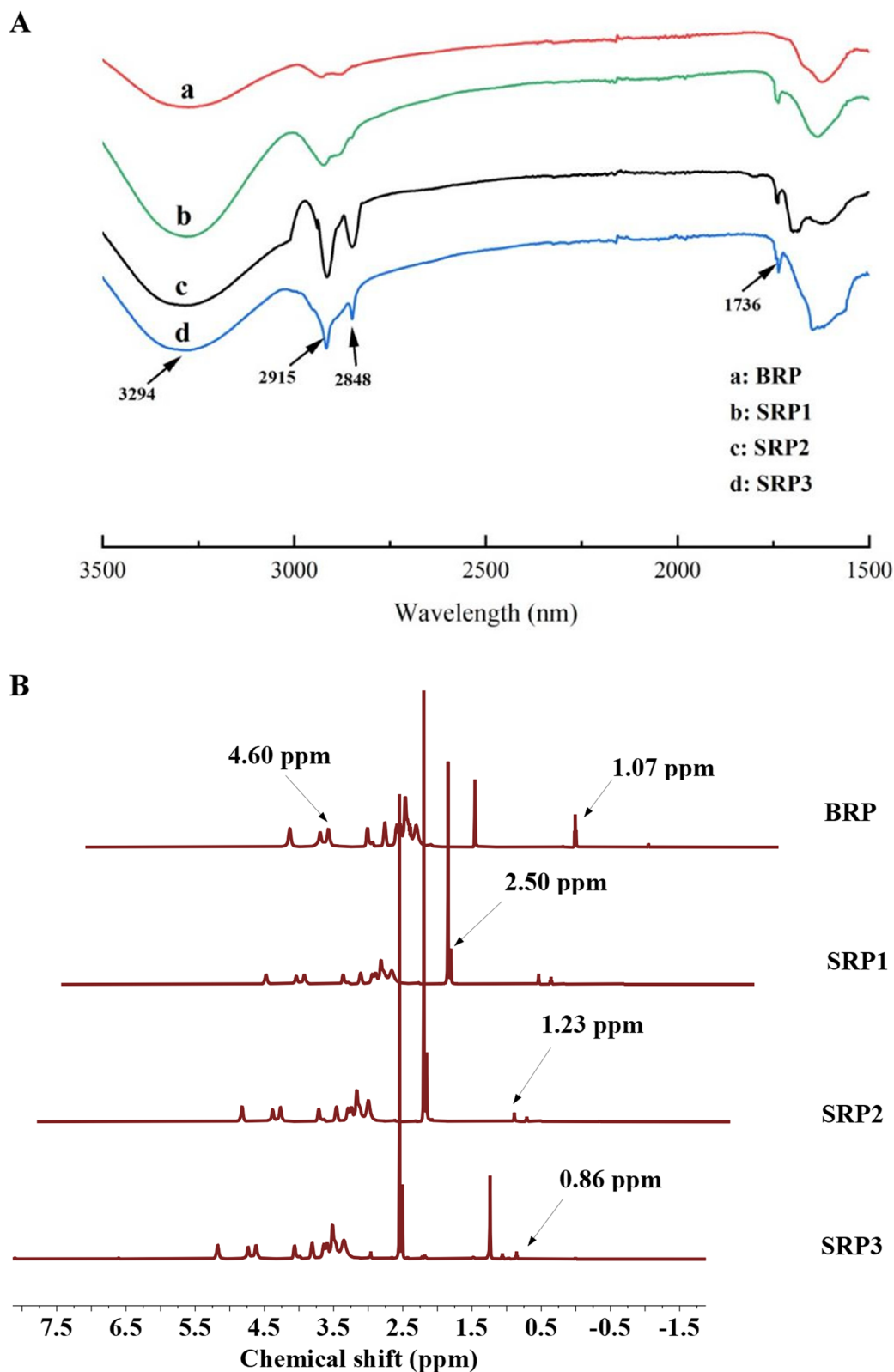


**Fig. 3** Infrared spectra (A) and <sup>1</sup>H NMR (B) of BRP and SA-modified BRP with different DS. BRP: Burdock root polysaccharide; SRP1: SA-modified BRP with the DS of 0.0239; SRP2: SA-modified BRP with the DS of 0.0488; SRP3: SA-modified BRP with the DS of 0.0883. The same as Figs. 4 and 5; Table 3

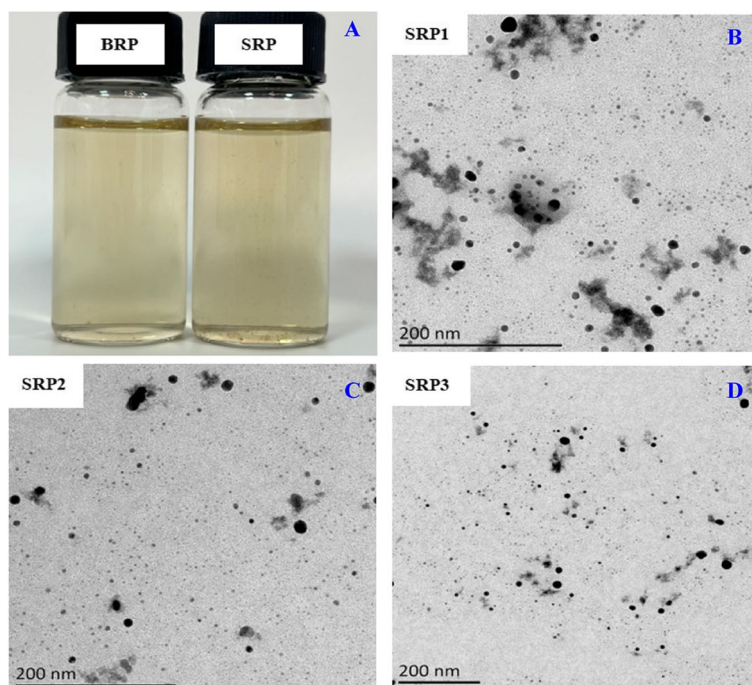


**Fig. 4** Observation on the morphology of self-aggregating micelles of SA-modified BRP. **A** appearance for BRP and SRP solutions; **B-D** TEM photographs for SRP1, SRP2 and SRP3

acyl chain of the SA molecule appeared at  $\delta$  0.86 ppm, as the degree of substitution increased, the peaks at the two positions gradually increased (Barrios et al. 2013). Additionally, the solvent peaks of DMSO-S6 around  $\delta$  2.50 ppm appeared as multiple peaks, which might be due to the presence of such methyl groups in the measured samples. By comparing the  $^1\text{H}$  NMR of BRP before and after modification, it was further proved that the hydrophobic side of SA was linked to the backbone of BRP, and the occurrence of esterification reaction was confirmed.

#### The morphology, particle size and solubility of SA-modified BRP micelles

It can be seen from Fig. 4 that the SA-modified BRP micelles with different DS were roughly spherical, with uniform particle size and high dispersibility, which might be related to the hydrophobic interaction between amphiphilic polysaccharide molecules (Gonçalves et al. 2007). The particle size of the self-aggregating micelles formed

by the SA-modified BRP ranged from 259 to 352 nm (Table 3), and decreased with increasing DS. It was due to the differences in specific surface area and surface energy under different DS in the micelle system formed by SA-modified BRP itself, resulting in different degrees of spontaneous particle aggregation. It was clear that the PDI of micelles formed by most amphiphilic polysaccharides was narrow. The smaller the PDI value, the more uniform the particle size distribution. When the PDI value is above 0.7, it represents a wide particle size distribution (Niu et al. 2022). The PDI values of SA-modified BRP micelles with different DS were less than 0.7, indicating that their particle size was relatively uniform and consistent with the apparent morphology presented by TEM. Moreover, the absolute zeta potential values of the SA-modified BRP micelles increased with the increase of DS, and were all greater than 20 mV, indicating that the stability of the self-aggregating micelles formed by SA-modified BRP was enhanced.

As shown in Table 3, the solubility of the SA-modified BRP was lower than that of the original BRP, decreased by 24.9–37.6%, and showed a certain negative correlation with the DS, indicating that the introduction of SA hydrophobic groups reduced the solubility of BRP. However, as the DS of SA-modified BRP increased, their solubility changed less, indicating that the degree of hydrophobic modification had a smaller impact on further reducing solubility.

**Table 3** The solubility of BRP and its derivatives

Item	BRP	SRP 1	SRP 2	SRP 3
Particle size/nm	-	352.4 ± 32.2	270.1 ± 22.6	259.6 ± 34.3
PDI	-	0.30	0.28	0.18
Zeta potential/ mV	-	-23.5	-28.1	-30.4
Solubility /%	98.1 ± 3.1	73.6 ± 2.4	62.1 ± 2.9	60.4 ± 1.5

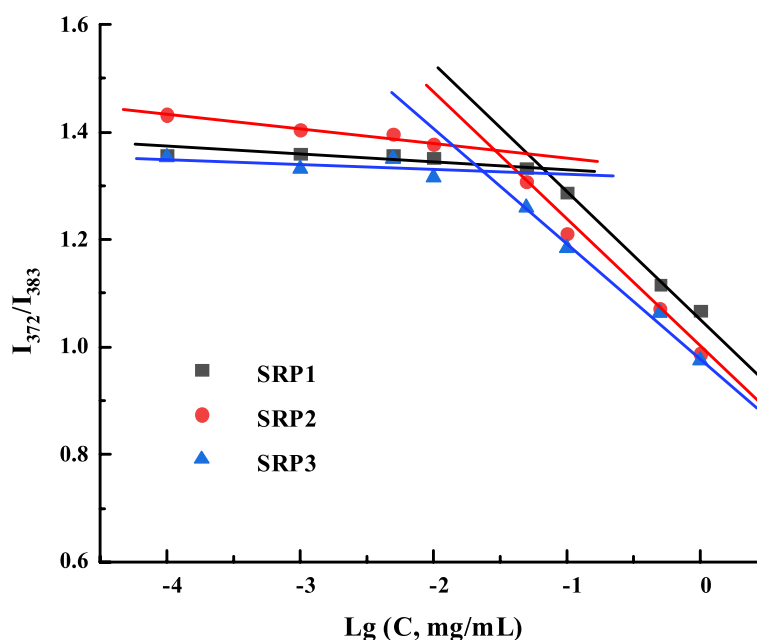


**Fig. 5** The relationship between the fluorescence intensity ratio of  $I_{372}/I_{383}$  from emission spectra of self-assembled micelles and the logarithm of concentration

#### CMC of SA-modified BRP micelles

CMC is commonly used to assess the ability of amphiphiles or surfactants to associate and form micelles in solution (Rapoport 2007; Mabrouk et al. 2022). Figure 5 shows the trend of the  $I_{372}/I_{383}$  ratio as a function of the mass concentration of SA-modified BRP. When the mass concentration of SA-modified BRP was low, the  $I_{372}/I_{383}$  ratio didn't obviously change. There was no micelle formation, and it existed in the form of a single chain. When the mass concentration of SA-modified BRP reached CMC, the  $I_{372}/I_{383}$  ratio decreased linearly with the increase of solution concentration. Pyrene molecules would enter the hydrophobic core of self-aggregated micelles and underwent strong reactions, indicating the formation of self-aggregated micelles (Qiu et al. 2014). Additionally, it was found that as the DS of SA-modified BRP increased, the CMC decreased, which was consistent with the results of Yang et al. (2021).

#### Conclusion

A novel amphiphilic BRP derivative modified by SA was synthesized through a simple esterification reaction. The optimal preparation conditions for SA-modified BRP were as follows: reaction time of 2 h, reaction temperature of 55 °C, system pH of 8.0 and the amount of SA added of 4 mmol, a maximum DS of the esterification products was obtained as 0.1012. Through FTIR analysis, it was observed the absorption peaks caused by

C-H stretching vibration at 2915  $\text{cm}^{-1}$  and 2848  $\text{cm}^{-1}$  of modified BRP derivatives were obviously enhanced compared with the unmodified sample. Moreover, a new peak was generated by ester carbonyl vibration at 1736  $\text{cm}^{-1}$ , proving that SA-modified BRP successfully introduced ester carbonyl and underwent esterification reaction, which was further confirmed by  $^1\text{H}$  NMR. The SA-modified BRP micelles were roughly spherical, evenly dispersed, and had a particle size in the range of 259–352 nm, which was negatively correlated with the degree of substitution. As the DS of esterification products increased, the absolute zeta potential values of micelle solutions were all above 20 mV, the kinetic stability was enhanced, while their solubility decreased to varying degrees. The CMC decreased leading to the formation of self-aggregating micelles. The above results indicated that SA-modified BRP could be used as a new carrier material for delivering hydrophobic active substances. We will next focus on exploring its loading capacity for hydrophobic active substances and potential mechanisms for improving their bioavailability.

#### Acknowledgements

Not applicable.

#### Authors' contributions

Chenchen Zhang: Manuscript writing, Methodology, Original research. Hongjuan Wang: Methodology, Review and Editing. Yan Zhang: Conceptualization, Review and Editing. Jiangfeng Song: Conceptualization, Original research, Review and Editing, Supervision. Ying Li: Editing. The author(s) read and approved the final manuscript.

## Funding

This work was supported by the project of Natural Science Foundation of Jiangsu Province (Project No. BK20201241) and Independent Innovation Fund Project of Agricultural Science and Technology in Jiangsu Province (Project No. CX (20)3047).

## Availability of data and materials

Research data will be shared on request by the corresponding author.

## Declarations

### Ethics approval and consent to participate

Not applicable.

### Consent for publication

Not applicable.

### Competing interests

The authors declare no conflict of interest.

## Author details

<sup>1</sup>Institute of Agro-product Processing, Jiangsu Academy of Agricultural Sciences, Nanjing 210014, China. <sup>2</sup>College of Food Science and Technology, Nanjing Agricultural University, Nanjing 210095, China.

Received: 14 August 2023 Accepted: 7 October 2023

Published online: 01 May 2024

## References

- Barrios, S. E., Giammanco, G., Contreras, J. M., Laredo, E., & López-Carrasquero, F. (2013). Characterization of esterified cassava starch with long alkyl side chains and different substitution degrees. *International Journal of Biological Macromolecules*, *59*, 384–390.
- Bu, X., Ji, N., Dai, L., et al. (2021). Self-assembled micelles based on amphiphilic biopolymers for delivery of functional ingredients. *Trends in Food Science & Technology*, *114*, 386–398.
- Chang, F., He, X., Fu, X., Huang, Q., & Qiu, Y. (2014). Preparation and characterization of modified starch granules with high hydrophobicity and flowability. *Food Chemistry*, *152*, 177–183.
- Chen, M., Liu, Y., Yang, W., et al. (2011). Preparation and characterization of self-assembled nanoparticles of 6-O-cholesterol-modified chitosan for drug delivery. *Carbohydrate Polymers*, *84*(4), 1244–1251.
- Gonçalves, C., Martins, J. A., & Gama, F. M. (2007). Self-assembled nanoparticles of dextrin substituted with hexadecanethiol. *Biomacromolecules*, *8*(2), 392–398.
- Hu, F. Q., Ren, G. F., Yuan, H., Du, Y. Z., & Zeng, S. (2006). Shell cross-linked stearic acid grafted chitosan oligosaccharide self-aggregated micelles for controlled release of paclitaxel. *Colloids and Surfaces B: Biointerfaces*, *50*(2), 97–103.
- Jeong, G. W., Jeong, Y. I., & Nah, J. W. (2019). Triggered doxorubicin release using redox-sensitive hyaluronic acid-g-stearic acid micelles for targeted cancer therapy. *Carbohydrate Polymers*, *209*, 161–171.
- Jiang, Y. Y., Yu, J., Li, Y. B., et al. (2019). Extraction and antioxidant activities of polysaccharides from roots of *Arctium lappa* L. *International Journal of Biological Macromolecules*, *123*, 531–538.
- Jin, X., Liu, S., & Chen, S. (2023). A systematic review on botany, ethnopharmacology, quality control, phytochemistry, pharmacology and toxicity of *Arctium lappa* L. fruit. *Journal of Ethnopharmacology*, *11*, 116223.
- Li, G., Xu, X., & Zhu, F. (2019). Physicochemical properties of dodecyl succinic anhydride (DDSA) modified quinoa starch. *Food Chemistry*, *300*, 125201.
- Li, H., Ma, Y., Yu, L., et al. (2020). Construction of octenyl succinic anhydride modified porous starch for improving bioaccessibility of  $\beta$ -carotene in emulsions. *RSC Advances*, *10*(14), 8480–8489.
- Li, L., Qiu, Z., Dong, H., Ma, C., Qiao, Y., & Zheng, Z. (2021). Structural characterization and antioxidant activities of one Neutral polysaccharide and three acid polysaccharides from the roots of *Arctium lappa* L.: A comparison. *International Journal of Biological Macromolecules*, *182*, 187–196.
- Lin, Q., Liang, R., Zhong, F., et al. (2019). Self-assembled micelles based on OSA-modified starches for enhancing solubility of  $\beta$ -carotene: Effect of starch macromolecular architecture. *Journal of Agricultural and Food Chemistry*, *67*(23), 6614–6624.
- Liu, C. M., Liang, R. H., Dai, T. T., et al. (2016). Effect of dynamic high pressure microfluidization modified insoluble dietary fiber on gelatinization and rheology of rice starch. *Food Hydrocolloids*, *57*, 55–61.
- Liu, C., Ning, R., Lei, F., Li, P., Wang, K., & Jiang, J. (2022). Study on the structure and physicochemical properties of fenugreek galactomannan modified via octenyl succinic anhydride. *International Journal of Biological Macromolecules*, *214*, 91–99.
- Lu, X., Luo, Z., Fu, X., & Xiao, Z. (2013). Two-step method of enzymatic synthesis of starch laurate in ionic liquids. *Journal of Agricultural and Food Chemistry*, *61*(41), 9882–9891.
- Ma, Y., Liu, J., Ye, F., & Zhao, G. (2016). Solubilization of  $\beta$ -carotene with oat  $\beta$ -glucan octenylsuccinate micelles and their freeze-thaw, thermal and storage stability. *LWT-Food Science and Technology*, *65*, 845–851.
- Mabrouk, M. M., Hamed, N. A., & Mansour, F. R. (2022). Physicochemical and electrochemical methods for determination of critical micelle concentrations of surfactants: A comprehensive review. *Monatshefte für Chemie-Chemical Monthly*, *153*(2), 125–138.
- Niu, B., Chen, H., Wu, W., et al. (2022). Co-encapsulation of chlorogenic acid and cinnamaldehyde essential oil in Pickering emulsion stabilized by chitosan nanoparticles. *Food Chemistry*, *371*, 100312.
- Perumal, S., Atchudan, R., & Lee, W. (2022). A review of polymeric micelles and their applications. *Polymers*, *14*(12), 2510.
- Qiu, L., Li, Z., Qiao, M., et al. (2014). Self-assembled pH-responsive hyaluronic acid-g-poly (L-histidine) copolymer micelles for targeted intracellular delivery of doxorubicin. *Acta Biomaterialia*, *10*(5), 2024–2035.
- Rapoport, N. (2007). Physical stimuli-responsive polymeric micelles for anti-cancer drug delivery. *Progress in Polymer Science*, *32*(8–9), 962–990.
- Shah, N. N., Soni, N., & Singhal, R. S. (2018). Modification of proteins and polysaccharides using dodecyl succinic anhydride: Synthesis, properties and applications—A review. *International Journal of Biological Macromolecules*, *107*, 2224–2233.
- Song, Y. L., Li, J. H., & Wang, R. L. (2016). Structure and solubility of gluten-polysaccharide conjugates. *Journal of the Chinese Cereals and Oils Association*, *31*(12), 125–131.
- Varavinit, S., Chaokasem, N., & Shobsngob, S. (2001). Studies of flavor encapsulation by agents produced from modified sago and tapioca starches. *Starch-Stärke*, *53*(6), 281–287.
- Wang, D., Yin, H., Xu, L., Meng, X., & Kang, T. (2023). Chemical characterization of polysaccharides from *Arctium lappa* root and its hepatoprotective effects on mice. *Journal of Functional Foods*, *103*, 105482.
- Wang, J. Y., Song, D. D., & Bao, Y. M. (2012). Preparation of self-assembled nanoparticles of stearic acid modified pullulan derivatives and their application as novel carriers of drug delivery. *Acta Chimica Sinica*, *70*(10), 1193.
- Yan, C., McClements, D. J., Zou, L., & Liu, W. (2019). A stable high internal phase emulsion fabricated with OSA-modified starch: An improvement in  $\beta$ -carotene stability and bioaccessibility. *Food & Function*, *10*(9), 5446–5460.
- Yang, W. Y., Zhang, Y., Li, F. F., & Huang, D. F. (2021). Preparation and characterization of self-aggregating micelles of oat polysaccharides modified with stearic acid. *Journal of Chinese Institute of Food Science and Technology*, *21*(4), 46–54.
- Yang, Y. M., Zhen, Z. J., Li, G. Q., & Zhang, R. T. (2022). Preparation and structure characterization of modified jujube polysaccharides. *Food Research & Development*, *43*(9), 8–14.

## Publisher's Note

Springer Nature remains neutral with regard to jurisdictional claims in published maps and institutional affiliations.